UNIVERSITY OF COPENHAGEN

Delayed insulin absorption correlates with alterations in subcutaneous depot kinetics in rats with dietinduced obesity

Gradel, Anna Katrina Jógvansdóttir; Porsgaard, Trine ; Brockhoff, Per Mikael Bruun; Seested, Torben; Lykkesfeldt, Jens; Refsgaard, Hanne H. F.

Published in:
Obesity Science & Practice

DOI:
10.1002/osp4.326

Publication date:
2019

Document version
Publisher's PDF, also known as Version of record

Citation for published version (APA):
Gradel, A. K. J., Porsgaard, T., Brockhoff, P. M. B., Seested, T., Lykkesfeldt, J., & Refsgaard, H. H. F. (2019). Delayed insulin absorption correlates with alterations in subcutaneous depot kinetics in rats with dietinduced obesity. *Obesity Science & Practice*, *5*(3), 281-288. https://doi.org/10.1002/osp4.326

 doi: 10.1002/osp4.326

ORIGINAL ARTICLE

Delayed insulin absorption correlates with alterations in subcutaneous depot kinetics in rats with diet-induced obesity

A. K. J. Gradel[1,2], T. Porsgaard[2], P. B. Brockhoff[3], T. Seested[2], J. Lykkesfeldt[1] and H. H. F. Refsgaard[2]

[1]Department of Veterinary and Animal Sciences, Section of Experimental Animal Models, Faculty of Health and Medical Sciences, University of Copenhagen, Frederiksberg, Denmark; [2]Global Drug Discovery, Novo Nordisk A/S, Måløv, Denmark; [3]Department of Applied Mathematics and Computer Science, Technical University of Denmark, Kgs. Lyngby, Denmark.

Received 25 September 2018; revised 17 December 2018; accepted 19 December 2018

Correspondence should be addressed to AKJ Gradel, Department of Veterinary and Animal Sciences, Section of Experimental Animal Models, Faculty of Health and Medical Sciences, Ridebanevej 9, University of Copenhagen, 1870 Frederiksberg, Denmark.
E-mail: aqo@novonordisk.com

Summary

Objective

Obesity is associated with delayed insulin absorption upon subcutaneous (s.c.) dosing in humans. The aim of this study was to investigate whether alterations in depot structure and kinetics of the s.c. injection depot contribute to this delay.

Methods

Rats fed a high-fat diet (HFD) and low-fat diet (LFD) were included in a series of insulin pharmacokinetic and imaging studies. Injection depots were visualized with micro X-ray computed tomography imaging upon s.c. administration of insulin aspart mixed with the contrast agent iomeprol, and insulin aspart exposure was measured by means of luminescent oxygen channelling immunoassay.

Results

Body weight and fat mass were increased in rats fed an HFD vs. LFD ($p < 0.05$), whereas the lean mass was not. The HFD group exhibited delayed insulin absorption from the s.c. tissue ($p < 0.001$). This delay was associated with smaller injection depots upon s.c. dosing ($p < 0.05$) and correlated with a slower depot disappearance from the s.c. tissue ($p < 0.05$) compared with the LFD group. Depot disappearance from the s.c. tissue was inversely correlated with body fat mass ($p < 0.05$).

Conclusions

Alterations in s.c. injection depot structure and kinetics may play a role in the obesity-associated delay in insulin absorption.

Keywords: Injection depot, insulin pharmacokinetics, obesity, subcutaneous administration.

Introduction

A number of factors have been reported to affect the rate of insulin absorption from the subcutaneous (s.c.) tissue and represent a source of pharmacokinetic variability in people using s.c. insulin therapy (1). Obesity has been associated with delayed insulin absorption upon s.c. dosing in humans (2–5). This may partly be explained by an obesity-associated decrease in s.c. blood flow (2,4,5). The negative correlation between obesity and decreased s.c. blood flow has been observed in both fasting (2,4–9) and postprandial states (7,8,10), where the latter is reflected by an attenuated rise in blood flow in response to an oral glucose load or a mixed meal. Both decreased capillary density (2,11) and impaired vasomotor function (6) are thought to contribute to the decrease in s.c. blood flow.

Other factors related to the s.c. micro-enviroment likely also influence the insulin absorption profile. Upon s.c. administration of insulin, an injection depot will form in the s.c. tissue. The distribution of this depot determines both the degree of depot dilution and the distance between the insulin molecules and the s.c. blood capillaries (12,13). Consequently, the more the depot distributes in the s.c. tissue, the faster it likely absorbs into the circulation. This notion is supported by our recent findings, where it was observed that larger size depots correlated with a faster depot disappearance and that the rate of depot disappearance correlated with insulin exposure in rats (14).

The aim of the present study was to investigate whether alterations in depot distribution and kinetics contribute to the obesity-associated delay in insulin absorption. The effect of obesity was investigated in rats fed a high-fat diet (HFD) as compared with rats fed a low-fat diet (LFD). The rats were included in a number of pharmacokinetic and micro X-ray computed tomography (μCT) studies, allowing us to investigate the link between depot kinetics and insulin pharmacokinetics (14). As a correlation between insulin pharmacokinetics and depot kinetics was expected (14), it was hypothesized that obesity would not only be associated with delayed insulin absorption but also result in delayed disappearance of the injection depot upon s.c. dosing.

Methods

Animals

All procedures performed in this study were approved by the Danish Animal Experiment Inspectorate.

Figure 1 shows an overview of the study design. Male Sprague Dawley rats (Charles River, Wilmington, Massachusetts, USA) fed either an HFD or LFD were included in the study. The rats fed an HFD received a diet containing 60% fat from weaning to 22 weeks and 45% fat from arrival at 22 weeks (D12492 and D12451, respectively), whereas rats fed an LFD received a diet containing 10% fat from weaning (D12450K, Research Diets, Inc., New Brunswick, NJ 08901, USA). The effect of diet on insulin absorption was investigated when the rats were 33–34 weeks of age. The rats were subjected to μCT scans at 36–38 weeks of age. Finally, intravenous (i.v.) insulin profiles were obtained from 39-week-old rats.

Body composition

Body lean and fat mass were determined in all rats using EchoMRI Body Composition Analyser (EchoMRI, Houston, TX, USA) (15) when the rats were 26 or 30 weeks of age (rats included in the neck and flank dosing studies, respectively). Animal weights were recorded throughout the study period.

Insulin absorption

Insulin absorption upon s.c. neck dosing was investigated in HFD and LFD rats (n = 22 and n = 10, respectively). Rats were s.c. dosed in the neck with 12-nmol insulin aspart (20-μL NovoRapid®, Novo Nordisk, DK-2880 Bagsværd), and the blood was collected from the sublingual vein at 5, 15 and 60 min post-dosing, enabling us to assess the insulin levels prior to, at and after the expected insulin peak plasma concentration (C_{max}) (14). This experiment was repeated five times for each rat, enabling us to assess the pharmacokinetic variability across the two diet groups (14).

Injection depot visualization

Eight rats from each diet group were included in a μCT study for depot visualization, as previously described (14). In short, rats were anaesthetized with isoflurane and subsequently dosed in the neck with 20-μL insulin aspart mixed in a ratio of 80/20 with the contrast agent iomeprol (Novorapid® and Iomerol 350®, Bracco Imaging Scandinavia, DK-2100 Copenhagen Ø). The rats were then subjected to μCT scans at 1, 3, 7 and 13 min post-dosing (Quantum XT, PerkinElmer, Waltham, USA), and insulin exposure was determined by collecting the blood from the tail at 5 and 15 min post-dosing. The experiment was repeated three times for each rat.

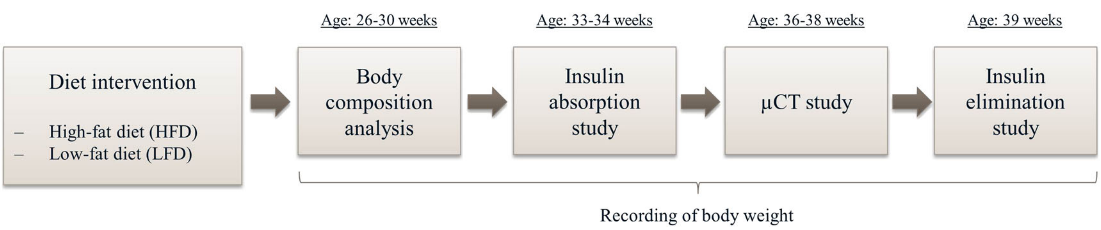

Figure 1 Study design. Male Sprague Dawley rats were fed either a high-fat diet (HFD, n = 29) or low-fat diet (LFD, n = 16) from weaning until the end of the study. Body composition was determined in all rats at week 26 and 30 (rats subcutaneous [s.c.] dosed in the neck and flank, respectively, in the insulin absorption/micro X-ray computed tomography [μCT] study). When rats were 33–34 weeks of age, the effect of diet on insulin absorption was investigated in rats fed an HFD (n = 22) and LFD (n = 10) upon s.c. administration of insulin aspart in the neck. All rats were subjected to μCT scans at 36–38 weeks of age where they were s.c. dosed in the neck (HFD, n = 8; LFD, n = 8) or flank (HFD, n = 7; LFD, n = 6) with insulin aspart mixed with iomeprol. Intravenous insulin aspart profiles were obtained from 39-week-old rats that had been dosed in the flank in the μCT study (HFD, n = 6; LFD, n = 6). Animal weight was recorded throughout the study period.

Based on the imaging results obtained from the rats dosed in the neck, a similar study was performed in rats dosed in the flank (HFD, n = 7; LFD, n = 6) following a similar protocol. This was done in order to investigate whether the findings on insulin pharmacokinetics and depot kinetics in the neck also apply to other injection regions. However, the scan time was prolonged to 17 min as a slower absorption rate upon flank dosing was expected (14). The experiment was repeated four times for each rat in order to increase study power, as fewer rats were included compared with the neck dosing μCT study. The rats dosed in the flank were selected based on body composition and weight so that similar differences in these parameters across the diet groups were obtained as in μCT study with neck dosing. I.v. insulin profiles were also investigated in these rats as described next.

Intravenous insulin profiles

To rule out potential differences in insulin clearance between rats in the two diet groups, i.v. insulin profiles were obtained from both diet groups in an insulin elimination study (HFD, n = 6; LFD, n = 6). All rats were anaesthetized with isoflurane prior to i.v. injection of insulin aspart (1 nmol kg^{-1}), and blood was collected from the tail at 3, 7, 15, 30, 60, 120 and 180 min post-dosing.

Biochemical analysis

Quantification of plasma insulin aspart was performed with luminescent oxygen channelling immunoassay technology (16).

Data handling and statistical analyses

Welch's t-test – or where applicable, Mann–Whitney test – was used to compare body weight and body composition between the diet groups. Statistical analyses of depots and insulin pharmacokinetics were performed as previously described (14): Volume and surface area of the injection depots detected on μCT scans were analysed in the imaging software Imaris (Bitplane AG, Zurich, Switzerland), and all repeated measurements of insulin exposure and depot structure were included in a mixed-model analysis with day and rat as random factors. The R-packages lme4 (17) and lmerTest (18) were used for the analysis. CT scans where the entire depot was not included (11 out of 397 scans) and pharmacokinetic profiles from unsuccessful dosings (four out of 260 dosings) were excluded from the statistical analyses. One rat was excluded from the analysis when evaluating the i.v. profiles of insulin aspart, as sample contamination was suspected. The correlation between fat mass and decrease in depot volume/surface area over time was investigated by means of linear regression analysis.

Statistical significance was defined by a p-value less than 0.05, and all data are reported as mean ± SEM. Means of repeated measurements in each group are figured as the mean of the averages from all rats. Because the depot volume and surface area were closely correlated (R^2 = 0.83, $p < 0.001$ by linear regression analysis) and thus generally yielded comparable results in terms of both depot kinetics and their correlation with insulin exposure, only depot volume data are included in the result section and figures. Finally, pharmacokinetic variability was estimated by simple methods by calculating the coefficient of variation (CV) for insulin exposure at 5, 15 and 60 min post-dosing for all rats and is reported as the mean CV% with 95% confidence interval.

Results

Body weight and composition

The HFD group had a significantly higher mean body weight compared with the LFD group throughout the study period: 777 ± 13 g vs. 658 ± 20 g and 869 ± 20 g vs. 731 ± 25 g when rats were 30 and 39 weeks of age, respectively ($p < 0.05$ or less). The mean fat mass was also significantly increased in the HFD group ($p < 0.001$, Figure 2a), whereas the mean lean mass was not.

Insulin pharmacokinetics

There was an effect of diet intervention on the pharmacokinetics of insulin aspart. This was reflected by significantly lower mean insulin concentration at 5, 15 and 60 min post-dosing and reduced area under the curve ($AUC_{0–60\ min}$, $p < 0.01$) in the HFD compared with the LFD group ($p < 0.001$, Figure 2b). Similar results were observed after weight-normalizing the insulin exposure ($p < 0.001$, Figure 2c). Despite injection region, the mean insulin concentration at 5 and 15 min post-dosing was also lower in the HFD group during the μCT scan studies when the rats were anaesthetized ($p < 0.05$ or less, Figure 2d). The injection region also had an effect on insulin pharmacokinetics, as rats dosed in the flank had a significantly lower mean insulin concentration compared with the rats dosed in the neck at 5 and 15 min ($p < 0.001$, Figure 2d).

The total variability in exposure (CV%) for the HFD and LFD groups at 5, 15 and 60 min was comparable:

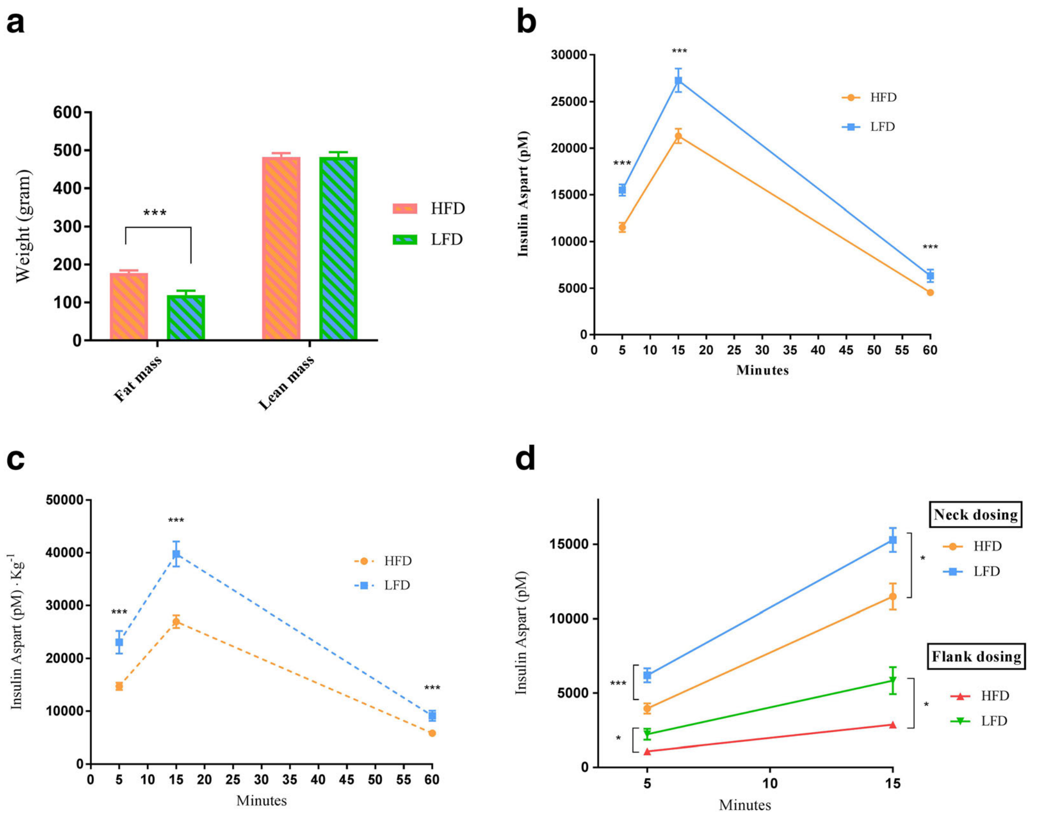

Figure 2 Body composition and insulin pharmacokinetics in rats fed a high-fat diet (HFD) or low-fat diet (LFD). (a) Body composition, fat and lean mass, in rats fed an HFD (n = 29) and LFD (n = 16). (b) Insulin aspart levels in Sprague Dawley rats fed an HFD (n = 22) and LFD (n = 10) upon subcutaneous (s.c.) administration of 20-μL (12-nmol) insulin aspart in the neck. (c) Insulin aspart levels after weight normalization in Sprague Dawley rats fed an HFD (n = 22) and LFD (n = 10) upon s.c. administration of 20-μL (12-nmol) insulin aspart in the neck. (d) Insulin aspart levels in HFD and LFD groups upon s.c. administration of 20-μL insulin aspart mixed with iomeprol in the neck (HFD, n = 8; LFD, n = 8) or flank (HFD, n = 7; LFD, n = 6). Data are shown as mean ± SE, and for the repeated measurements group, means are figured as the mean of the averages from all rats (b–d). $^{**}p < 0.01$, $^{***}p < 0.001$ by Welch's *t*-test or Mann–Whitney analysis (a) or repeated mixed-model analysis with day and rat as random factors (b–d).

29 [23; 34] vs. 35 [29; 40], 23 [19; 28] vs. 26 [18; 33] and 37 [31; 43] vs. 40 [25; 56].

Evaluating the i.v. profiles of insulin aspart from the two diet groups, no significant differences in a number of pharmacokinetic parameters were found across the diet groups, including the insulin concentrations at all sampling time points, the volume of distribution (V_d), the clearance rate (Cl_B) and the eliminations half-life ($T_{½}$, data not shown). Thus, the i.v. pharmacokinetic profiles of insulin aspart seem to be comparable between the two diet groups.

Depot kinetics

Examples of injection depots detected in an HFD and LFD rat are shown in Figure 3a. As previously observed, the highest concentration of iomeprol was located in the centre of the injection depot upon s.c. dosing (14). Figure 3b shows the changes in mean depot volume over time in rats s.c. dosed in the neck, where it is evident that the depot volume declines over time in both diet groups. However, compared with the LFD group, the injection depots in the HFD were initially smaller in size, reflected by a significantly smaller mean depot volume at 1 min post-dosing ($p < 0.01$). Moreover, these depots disappeared slower from the s.c. tissue, as measured by a smaller mean decrease in depot volume over time in the HFD group ($\Delta Vol_{1-3\ min}$, $\Delta Vol_{1-7\ min}$ and $\Delta Vol_{1-13\ min}$, $p < 0.05$ or less).

Similar findings were observed when the rats were dosed in the flank where the HFD group had significantly smaller mean depot volumes at 1 and 3 min, larger mean depot volumes at 13 and 17 min post-dosing and a smaller mean decrease in depot volume over time ($\Delta Vol_{1-7\ min}$, $\Delta Vol_{1-13\ min}$ and $\Delta Vol_{1-17\ min}$, $p < 0.05$, Figure 3c).

Despite diet group, the depot distribution and kinetics differed across the two injection regions. This was

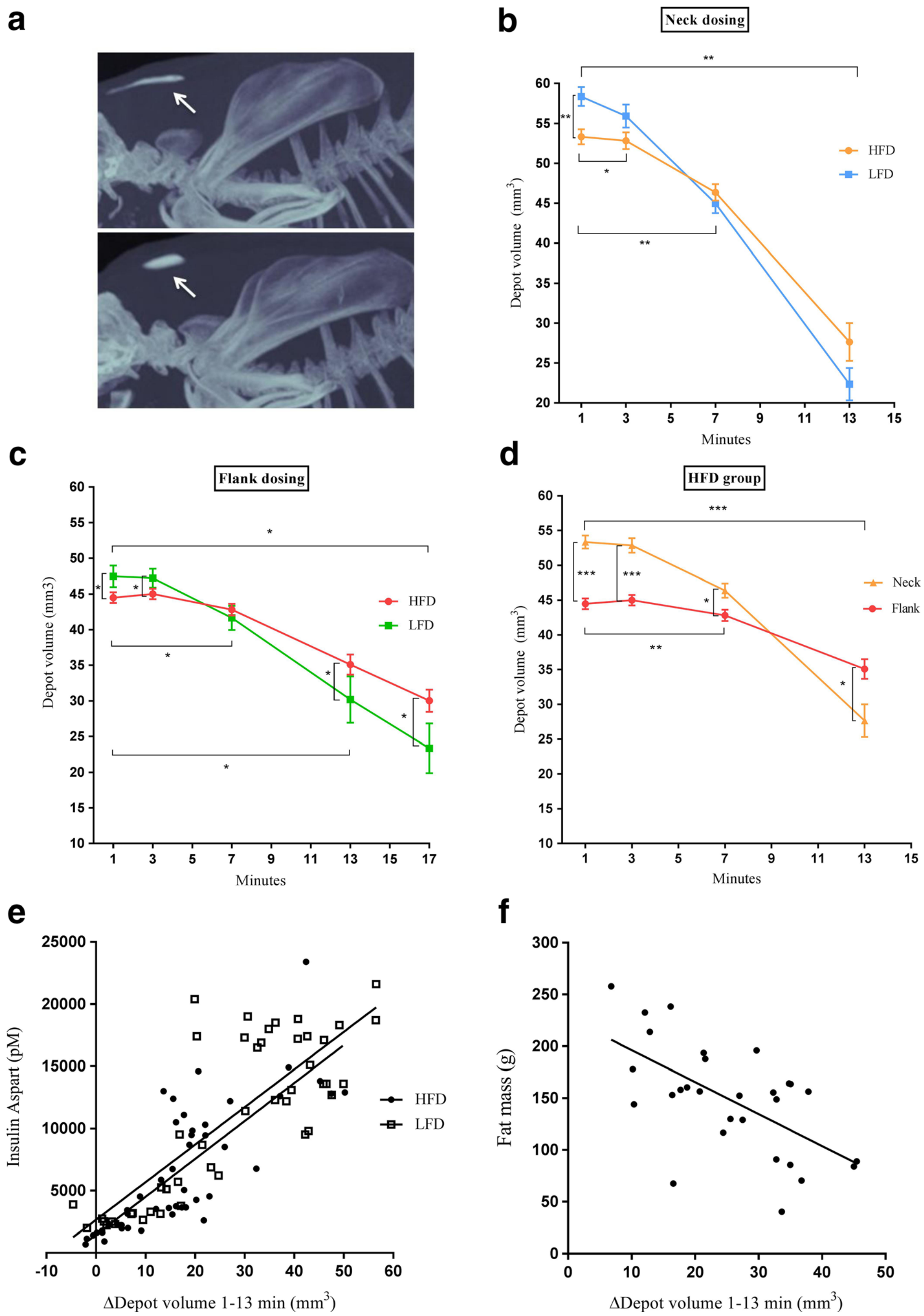

Figure 3 Injection depot kinetics and correlation with insulin pharmacokinetics in rats fed a high-fat diet (HFD) or low-fat diet (LFD). (a) Arrows on computed tomography images show subcutaneous (s.c.) neck depots from rats either fed an LFD (top: 60.6 mm^3 in size) or HFD (bottom: 53.5 mm^3 in size) at 1 min post-dosing with 20-μL insulin aspart mixed with iomeprol. (b) Depot volume over time in rats fed an HFD (n = 8) or LFD (n = 8) upon s.c. administration of 20-μL insulin aspart mixed with iomeprol. (c) Depot volume over time in rats fed an HFD (n = 8) or LFD (n = 8) upon s.c. administration of 20-μL insulin aspart mixed with iomeprol. (d) Depot volume over time in all rats fed an HFD (n = 8 and n = 7 for neck and flank dosing, respectively) upon s.c. administration of 20-μL insulin aspart mixed with iomeprol. For the LFD animals, see profiles in Figure 2b,c. (e) Decrease in depot volume over time ($\Delta Vol_{1\text{–}13\ min}$) was positively correlated with the insulin aspart levels at 15 min post-dosing in LFD (n = 14) and HFD (n = 15) rats upon s.c. administration of 20-μL insulin aspart mixed with iomeprol ($p < 0.001$ by repeated mixed-model analysis with day and rat as random factors). (f) Fat mass was negatively correlated with the average decrease in depot volume over time ($\Delta Vol_{1\text{–}13\ min}$) in rats subjected to micro X-ray computed tomography scans and s.c. dosed with 20-μL insulin aspart mixed with iomeprol (n = 29, $p < 0.001$ by linear regression analysis). Data in (b) to (d) are shown as mean ± SE, and means are figured as the mean of the averages from all rats. $^{**}p < 0.01$, $^{***}p < 0.001$ by repeated mixed-model analysis with day and rat as random factors (b–d).

reflected by initially smaller depot volume and slower depot disappearance in rats dosed in the flank vs. the neck ($p < 0.05$ or less, Figure 3d for the HFD animals).

In order to assess whether the initial depot distribution had an influence on the depot disappearance rate, the link between depot volume at 1 min post-dosing and the decrease in depot volume over time was investigated. Results showed a significant correlation between initial depot volume and the depot volume over time, irrespective of diet group and dosing region ($Vol_{1\ min}$ vs. $\Delta Vol_{1-13\ min}$ and $Vol_{1\ min}$ vs. $\Delta Vol_{1-17\ min}$, $p < 0.01$, data not shown).

There was a significant correlation between the speed of depot disappearance and the insulin concentration, irrespective of injection region and diet group ($\Delta Vol_{1-3\ min}$ vs. insulin 5 min, $p < 0.05$ or less; $\Delta Vol_{1-13\ min}$ vs. insulin 15 min, $p < 0.001$, Figure 3e). Thus, the faster the depot disappeared from the s.c. tissue, the higher the insulin exposure. Finally, it was also found that the average depot disappearance rate was negatively correlated with the total body fat mass, i.e. the higher the fat mass, the slower the depot disappeared from the s.c. tissue (neck dosing: $p < 0.05$ and $R^2 = 0.28$; flank dosing: $p < 0.01$ and $R^2 = 0.64$; all dosings: $p < 0.001$ and $R^2 = 0.37$, Figure 3f).

Discussion

Feeding of a diet rich in fat has been reported to be accompanied by an expansion in adipose tissue mass in rats (19–22). Accordingly, it was observed that rats fed an HFD had a significantly higher body weight and fat mass compared with rats fed an LFD, whereas the lean mass was comparable across the diet groups, indicating that the diet intervention used in this study can be used to assess the effect of obesity on insulin pharmacokinetics and depot structure in rats.

As reported in people with obesity (2–5), a delayed insulin absorption was also observed in the rats fed an HFD in this study. This may partly be attributed to alterations in the distribution and kinetics of the injection depot, because the depots from rats fed an HFD were both smaller in size (indicating a smaller distribution upon s.c. dosing) and disappeared slower from the s.c. tissue, as measured by a smaller decrease in depot volume over time. The more an injection depot distributes in the s.c. compartment, the shorter the distance will likely be for insulin to be absorbed by blood capillaries, because insulin needs to travel through the extracellular matrix prior to trans-capillary transport. An increased depot distribution is also believed to result in increased and faster dilution of the injection depot, thus yielding a higher concentration of insulin monomers and dimers that are associated with a faster absorption compared with insulin hexamers, as previously discussed (13,14,23). Therefore, it may not be surprising that a significant positive correlation between the initial depot size and the speed of depot disappearance was found (the larger the depot, the faster the depot disappearance) and between the speed of depot disappearance and insulin exposure (the faster the depot disappears, the faster insulin is absorbed into the circulation). Thus, the depot structure and kinetics detected on the CT scans can be used to predict the insulin exposure and may partly explain the obesity-associated delay in insulin absorption. The fact that a slow depot disappearance is linked to adipose tissue mass is supported by the finding of a negative correlation between body fat mass and the speed of depot disappearance from the s.c. tissue.

Although the CT scans in this study only detect the distribution of the contrast media and not of insulin aspart, a correlation between depot kinetics and insulin exposure was observed. Furthermore, a similar distribution of insulin aspart and another non-ionic water-soluble contrast agent has been reported in pig s.c. tissue, as previously discussed (14,24). Thus, it is reasonable to assume that depots detected on the CT represent the insulin injection depot.

Obesity is known to result in expansion of the adipose tissue in both humans and rodents, occurring as a result of adipocyte hypertrophy, hyperplasia or a combination of both depending on the region of interest (20,21,25–27). Obesity could therefore be speculated to increase the adipose tissue to interstitial fluid ratio in the s.c. compartment, which to a larger degree may limit the distribution of insulin aspart in the s.c. tissue, since the insulin aspart preparation is hydrophilic and thus likely only distributes in the interstitial fluid upon s.c. dosing. In addition to limiting depot distribution, an expansion of the adipose tissue mass in rats with diet-induced obesity may also result in reduced s.c. blood flow, likely as a result of reduced capillary density and consequently capillary area available for insulin diffusion, which may delay depot disappearance and consequently insulin absorption. Furthermore, it still remains to be determined whether these rats have impaired vasomotor function. Blood flow measurements and tissue characterization could thus be relevant for future studies in order to differentiate between the relative contribution of s.c. blood flow, injection depot structure or additional factors to the delayed depot disappearance/insulin absorption.

Irrespective of diet group, injection into the neck vs. the flank was associated with faster insulin absorption. Furthermore, the regional differences in insulin pharmacokinetics also correlated with depot kinetics. In humans, s.c. administration of insulin into the arm or abdomen is associated with an accelerated absorption compared with administration into the thigh, irrespective of body weight (2,28–31). Thus, as in humans with obesity, rats fed an HFD not only exhibit a delayed insulin absorption upon s.c. dosing, but the regional differences in insulin pharmacokinetics are maintained (2). We have previously found similar regional differences in insulin pharmacokinetics and depot kinetics in Sprague Dawley rats receiving standard chow (14), indicating that this phenomenon may occur irrespective of diet choice/obesity status.

When considering the impact of the insulin injection depot on insulin pharmacokinetics, this study supports how improvements in pharmaceutical formulation or administration technique can be used to diminish the obesity-associated delay in insulin absorption. Although their use is limited in the diabetic community, devices such as jet injectors allow for the insulin depot to be dispersed in a spray-like manner in the s.c. tissue, thus increasing its distribution. Accordingly, jet injectors have been reported to be associated with beneficial effect in people with obesity because the pharmacokinetic profile of insulin to a lesser degree is affected by the insulin dose or body weight (3). Simpler techniques that can be used to facilitate a more rapid insulin absorption include a dispersed injection strategy (32) or local massage of the injection site (33,34). Adding excipients such as hyaluronidase (35,36) or biochaperone (37) to the insulin formulation also represents another mechanism by which the depot distribution and diffusion in the s.c. tissue can be enhanced. These strategies may all facilitate a faster absorption from the s.c. tissue and consequently a faster glucose-lowering effect in people with obesity.

Conclusion

In addition to increased body weight and fat mass, rats fed an HFD exhibited delayed insulin absorption upon s.c. dosing compared with rats fed an LFD. This delay was associated with decreased depot distribution upon s.c. dosing and correlated with a slower depot disappearance. Thus, differences in depot structure and kinetics may contribute to the obesity-associated delay in insulin absorption.

Acknowledgements

We would sincerely like to thank laboratory technician Emilie Due Jensen for her dedicated assistance in obtaining blood samples to be used for pharmacokinetic profiling and Dr. Valentina Manfè for quantifying insulin aspart levels in plasma samples. We also would like to thank Lars Hovgaard and Christina Rose Petersen for assisting in the formulation of the insulin aspart/iomeprol formulation. Finally, we would like to thank Drs Jeppe Sturis and Christian Fledelius for their input in the interpretation of the CT scan data.

Funding

This work was funded in part by The LifePharm Centre for In Vivo Pharmacology at University of Copenhagen (A. K. J. G. and J. L.) and by Novo Nordisk A/S.

Conflict of Interest Statement

All authors declare no conflict of interest in relation to the present work.

References

1. Gradel AKJ, Porsgaard T, Lykkesfeldt J, et al. Factors affecting the absorption of subcutaneously administered insulin: effect on variability. *J Diabetes Res* 2018; **2018**. https://doi.org/10.1155/2018/1205121: 1–17.
2. Vora JP, Burch A, Peters JR, Owens DR. Relationship between absorption of radiolabeled soluble insulin, subcutaneous blood flow, and anthropometry. *Diabetes Care* 1992; **15**: 1484–1493.
3. De Galan BE, Engwerda EEC, Abbink EJ, Tack CJ. Body mass index and the efficacy of needle-free jet injection for the administration of rapid-acting insulin analogs, apost hocanalysis. *Diabetes Obes Metab* 2013; **15**: 84–86. https://doi.org/10.1111/j.1463-1326.2012.01666.x.
4. Hildebrandt P. Skinfold thickness, local subcutaneous blood flow and insulin absorption in diabetic patients. *Acta Physiol Scand* 1991; **603**: 41–45.
5. Sindelka G, Heinemann L, Berger M, Frenck W, Chantelau E. Effect of insulin concentration, subcutaneous fat thickness and skin temperature on subcutaneous insulin absorption in healthy subjects. *Diabetologia* 1994; **37**: 377–380.
6. Blaak EE, van Baak MA, Kemerink GJ, Pakbiers MTW, Heidendal GAK, Saris WHM. β-Adrenergic stimulation and abdominal subcutaneous fat blood flow in lean, obese, and reduced-obese subjects. *Metabolism* 1995; **44**: 183–187.
7. Jansson PAE, Larsson A, Lönnroth PN. Relationship between blood pressure, metabolic variables and blood flow in obese subjects with or without non-insulin-dependent diabetes mellitus. *Eur J Clin Invest* 1998; **28**: 813–818. https://doi.org/10.1046/j.1365-2362.1998.00360.x.
8. Summers LKM, Samra JS, Humphreys SM, Morris RJ, Frayn KN. Subcutaneous abdominal adipose tissue blood flow: variation within and between subjects and relationship to obesity. *Clin Sci* 1996; **91**: 679–683.
9. Frayn KN, Humphreys SM. Metabolic characteristics of human subcutaneous abdominal adipose tissue after overnight fast. *Am J Physiol Endocrinol Metab* 2012; **302**: E468–E475. https://doi.org/10.1152/ajpendo.00527.2011.
10. Tobin L, Simonsen L, Bülow J. The dynamics of the microcirculation in the subcutaneous adipose tissue is impaired in the postprandial state in type 2 diabetes. *Clin Physiol Funct Imaging* 2011; **31**: 458–463. https://doi.org/10.1111/j.1475-097X.2011.01041.x.
11. Goossens GH, Bizzarri A, Venteclef N, et al. Increased adipose tissue oxygen tension in obese compared with lean men is accompanied by insulin resistance, impaired adipose tissue capillarization, and inflammation. *Circulation* 2011; **124**: 67–76. https://doi.org/10.1161/CIRCULATIONAHA.111.027813.

12. Kang S, Brange J, Burch A, Vølund A, Owens DR. Subcutaneous insulin absorption explained by insulin's physicochemical properties. Evidence from absorption studies of soluble human insulin and insulin analogues in humans. *Diabetes Care* 1991; **14**: 942–948.
13. Søeborg T, Rasmussen CH, Mosekilde E, Colding-Jørgensen M. Absorption kinetics of insulin after subcutaneous administration. *Eur J Pharm Sci* 2009; **36**: 78–90. https://doi.org/10.1016/j.ejps.2008.10.018.
14. Gradel AKJ, Porsgaard T, Lykkesfeldt J, Brockhoff P, Seested T, Refsgaard H. Subcutaneous administration of insulin is associated with regional differences in injection depot variability and kinetics in the rat. *Exp Clin Endocrinol Diabetes* 2018 https://doi.org/10.1055/a-0658-1089.
15. Metzinger MN, Miramontes B, Zhou P, et al. Correlation of X-ray computed tomography with quantitative nuclear magnetic resonance methods for pre-clinical measurement of adipose and lean tissues in living mice. *Sensors* 2014; **14**: 18526–18542. https://doi.org/10.3390/s141018526.
16. Petersen SB, Lovmand JM, Honoré L, Jeppesen CB, Pridal L, Skyggebjerg O. Comparison of a luminescent oxygen channeling immunoassay and an ELISA for detecting insulin aspart in human serum. *J Pharm Biomed Anal* 2010; **51**: 217–224. https://doi.org/10.1016/j.jpba.2009.08.008.
17. Bates D, Mächler M, Bolker BM, Walker SC. Fitting linear mixed-effects models using lme4. *J Stat Softw* 2015; **67** https://doi.org/10.18637/jss.v067.i01.
18. Kuznetsova A, Brockhoff PB, Christensen RHB. lmerTest package: tests in linear mixed effects models. *J Stat Softw* 2017; **82**: 1–26. https://doi.org/10.18637/jss.v082.i13.
19. Storlien LH, James DE, Burleigh KM, Chisholm DJ, Kraegen EW. Fat feeding causes widespread in vivo insulin resistance, decreased energy expenditure, and obesity in rats. *Am J Physiol Endocrinol Metab* 1986; **251**: E576–E583. https://doi.org/10.1152/ajpendo.1986.251.5.e576.
20. Lemonnier D. Effect of age, sex, and site on the cellularity of the adipose tissue in mice and rats rendered obese by a high-fat diet. *J Clin Invest* 1972; **51**: 2907–2915.
21. Berger JJ, Barnard RJ. Effect of diet on fat cell size and hormone-sensitive lipase activity. *J Appl Physiol* 1999; **87**: 227–232.
22. Zaragoza-Hermans N, Felber JP. Studies of the metabolic effects induced in the rat by a high fat diet – II. Disposal of orally administered (14C)-glucose*. *Horm Metab Res* 1972; **4**: 25–30.
23. Rasmussen CH, Røge RM, Ma Z, et al. Insulin aspart pharmacokinetics: an assessment of its variability and underlying mechanisms. *Eur J Pharm Sci* 2014; **62**: 65–75. https://doi.org/10.1016/j.ejps.2014.05.010.
24. Thomsen M, Rasmussen CH, Refsgaard HH, et al. Spatial distribution of soluble insulin in pig subcutaneous tissue: effect of needle length, injection speed and injected volume. *Eur J Pharm Sci* 2015; **79**: 96–101. https://doi.org/10.1016/j.ejps.2015.08.012.
25. Tchoukalova YD, Votruba SB, Tchkonia T, Giorgadze N, Kirkland JL, Jensen MD. Regional differences in cellular mechanisms of adipose tissue gain with overfeeding. *PNAS* 2010; **107**: 18226–18231.
26. Muir LA, Neeley CK, Meyer KA, et al. Adipose tissue fibrosis, hypertrophy, and hyperplasia: correlations with diabetes in human obesity. *Obesity* 2016; **24**: 597–605. https://doi.org/10.1002/oby.21377.
27. Rutkowski JM, Stern JH, Scherer PE. The cell biology of fat expansion. *J Cell Biol* 2015; **208**: 501–512. https://doi.org/10.1083/jcb.201409063.
28. Mudaliar SR, Lindberg FA, Joyce M, et al. Insulin aspart (B28 asp-insulin): a fast-acting analog of human insulin: absorption kinetics and action profile compared with regular human insulin in healthy nondiabetic subjects. *Diabetes Care* 1999; **22**: 1501–1506.
29. Galloway JA, Spradlin CT, Nelson RK, Wentworth SM, Davidson JA, Swarner JL. Factors influencing the absorption, serum insulin concentration, and blood glucose responses after injections of regular insulin and various insulin mixtures. *Diabetes Care* 1981; **4**: 366–376.
30. Braak EWT, Woodworth JR, Bianchi R, et al. Injection site effects on the pharmacokinetics and glucodynamics of insulin lispro and regular insulin. *Diabetes Care* 1996; **19**: 1437–1440.
31. Hövelmann U, Heise T, Nosek L, Sassenfeld B, Thomsen KMD, Haahr H. Pharmacokinetic properties of fast-acting insulin aspart administered in different subcutaneous injection regions. *Clin Drug Investig* 2017; **37**: 503–509. https://doi.org/10.1007/s40261-017-0499-y.
32. Mader JK, Birngruber T, Korsatko S, et al. Enhanced absorption of insulin aspart as the result of a dispersed injection strategy tested in a randomized trial in type 1 diabetic patients. *Diabetes Care* 2013; **36**: 780–785. https://doi.org/10.2337/dc12-1319.
33. Dillon RS. Improved serum insulin profiles in diabetic individuals who massaged their insulin injection sites. *Diabetes Care* 1983; **6**: 399–401.
34. Linde B. Dissociation of insulin absorption and blood flow during massage of a subcutaneous injection site. *Diabetes Care* 1986; **9**: 570–574.
35. Hompesch M, Muchmore DB, Morrow L, Vaughn DE. Accelerated insulin pharmacokinetics and improved postprandial glycemic control in patients with type 1 diabetes after coadministration of prandial insulins with hyaluronidase. *Diabetes Care* 2011; **34**: 666–668. https://doi.org/10.2337/dc10-1892.
36. Hompesch M, Muchmore DB, Morrow L, Ludington E, Vaughn DE. Improved postprandial glycemic control in patients with type 2 diabetes from subcutaneous injection of insulin lispro with hyaluronidase. *Diabetes Technol Ther* 2012; **14**: 218–224. https://doi.org/10.1089/dia.2011.0117.
37. Andersen G, Alluis B, Meiffren G, Ranson, A, Seroussi, C, Soula, O, Fischer, A, Nosek, L, Schliess, F, Heise, T The ultra-rapid biochaperone insulin lispro shows a faster onset of action and stronger early metabolic effect than insulin lispro alone [Web page] Accessed August 31, 2018. https://www.adocia.com/wp-content/uploads/2016/03/140624-Poster-BC-Lispro-ADA-74th-final_VF_ADOCIA.pdf.